On the Dynamic Stability of OTEC Cold Water Pipe (CWP) under Variations of Force Balance Descriptions at the Free Inlet

Adiputra, Ristiyanto
Research Center for Hydrodynamics Technology, National Research and Innovation Agency, Indonesia

Muhammad Iqbal Habib
Department of Mechanical Engineering, Universitas Sebelas Maret

Rahuna, Daif
Research Center for Hydrodynamics Technology, National Research and Innovation Agency, Indonesia

Muttaqie, Teguh
Research Center for Hydrodynamics Technology, National Research and Innovation Agency, Indonesia

他

https://doi.org/10.5109/7151716

出版情報：Evergreen. 10 (3), pp.1674-1682, 2023-09. 九州大学グリーンテクノロジー研究教育センター
バージョン：

On the Dynamic Stability of OTEC Cold Water Pipe (CWP) under Variations of Force Balance Descriptions at the Free Inlet

Ristiyanto Adiputra[1,*], Muhammad Iqbal Habib[2], Daif Rahuna[1], Teguh Muttaqie[1], Erwandi[1], Aditya Rio Prabowo[2,*], Cahyadi Sugeng Jati Mintarso[1]

[1]Research Center for Hydrodynamics Technology, National Research and Innovation Agency, Indonesia

[2]Department of Mechanical Engineering, Universitas Sebelas Maret, Indonesia

*Author to whom correspondence should be addressed:
E-mail: ristiyanto.adiputra@brin.go.id; aditya@ft.uns.ac.id

(Received February 14, 2023; Revised June 1, 2023; accepted June 13, 2023).

Abstract: Ocean Thermal Energy Conversion (OTEC) Cold Water Pipe (CWP) can be addressed as a riser conveying fluid which is predicted to be unstable when the internal velocity exceeds its critical value. However, the numerical analysis shows a momentum change at the free inlet, which may influence the riser stability. Thus, this paper analyzed the stability of OTEC CWP analytically by considering the force balance at the inlet. The modeling of the pipe and the variations in force balance modeling were conducted using the finite element method where the pipe stability behavior was assessed by observing the displacement of the last node of the pipe over time generated via the Newmark time scheme method. The critical velocity on a small-scale fixed joint pipe model, including shear force balance, was 5.06 m/s, while the critical velocity with partial shear force balance and no shear force balance was between 2.3-2.4 m/s. In the full-scale model, the critical velocity with shear force balance was 5 m/s and 4.75 m/s, for fixed joint and pinned joint, respectively. Critical velocity generated by partially and fully excluding shear force balance on the pipe model is 3.66 m/s and 3.68 m/s for the fixed joint and 3.58 and 3.62 for the pinned joint. The results showed that the inclusion of shear force balance increased the critical velocity.

Keywords: Ocean Thermal Energy Conversion (OTEC); Cold Water Pipe (CWP); riser conveying fluid, Finite Element Method (FEM), Internal Flow Effect (IFE)

1. Introduction

Ocean Thermal Energy Conversion (OTEC) is a method to harvest solar energy stored in the ocean by employing the temperature difference between surface and deep seawater[1)]. The temperature difference must exceed 20^{O}C for viable utilization[2)]. Thus, OTEC resources mainly locate in countries with tropical or subtropical climates[3)]. To produce 100 MW-net electricity, the Cold-Water Pipe (CWP) component is attached to a floating platform to draw cold seawater from approximately 800[4)]-1000[5)] meters of water depth.

The previous plant design required CWP with a 12 m diameter to transport 235 m^3/s of deep cold seawater[6)]. Recent studies indicated that with current technology, the maximum diameter of the riser possibly attached to the OTEC powerplant was only 3 m due to manufacturing capability limitations. Thus, obtaining a similar net power target required the installation of multiple pipes[7)].

The concept of the previously proposed OTEC floating platform was adapted, and the front-view configuration was visualized, as shown in Fig. 1[8)]. The pipe is installed in a free-hanging configuration which is very challenging as this typical configuration is very fragile toward the applied loads such as vortex-induced vibration[9)], Internal Flow Effects[10)], and plantship motion[11)]. Several studies related to OTEC CWP as a submerged riser conveying fluid can be seen in Table 1.

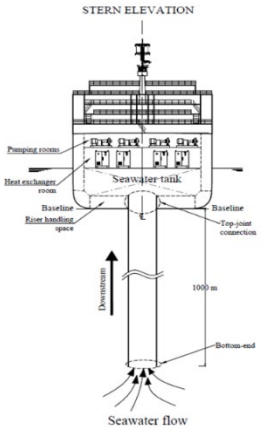

Fig. 1: OTEC CWP configuration[8)]

Table 1. Milestone Study

Reference	Objective	Method	Results
1 [7]	Presenting analytical and numerical analyses of OTEC CWP subjected to internal flow effect (IFE) and ambient fluid effects (added mass and drag force). Analysis using non-linear and linear differential equations is employed.	Analytical Method (Galerkin Method) and Numerical Method (Finite Element Method)	Numerical simulation was in a good agreement with the analytical analysis.
2 [8]	Determining design for OTEC CWP define as a riser conveying fluid considering internal flow effect and boundary condition	Analytical Method and Numerical Method	Numerical and analytical result was compared. Top joint connection, pipe inlet clump, and pipe material were varied.
3 [12]	Presenting a numerical method for predicting the response of a cantilevered tube conveying fluid, neglecting tube rotary inertia.	Numerical Method (FEM)	The experimental data and numerical results agreed well qualitatively.
4 [13]	Presenting Finite element model of pipe conveying fluid and observing pipe behavior to determine design improvement and optimization.	Numerical Method (FEM)	Improvement increased critical velocity by 74.5 percent to 10.14 m/s.
5 [14]	Investigating the dynamic response of marine riser to top-end excitation.	Finite Element Method and Newmark Average Acceleration Method.	Beating and resonance phenomenon was observed
6 [15]	Analyzing the stability of OTEC CWP using the Finite Element Method. Considering centrifugal and coriolis force.	Semi-analytical Method using Finite element model. In Time domain	The critical velocity obtained from the analysis was around 4.5-4.8 m/s.
7 [16]	Provide an experiment to take a new look at the dynamics of pipe-aspirating fluid (water)	Experimental	Pipe at small scale still in stable condition at 2 m/s fluid velocity

Because OTEC is in the early development stage, there are still a lot of uncertainties, including the design of OTEC CWP [17]. As shown in Table 1, the effect of the force balance at the inlet has not been comprehensively included in the internal flow effects analysis for OTEC CWP. Considering this, this paper analyzes the change of critical velocity due to the variations in the description of force balance at the free inlet considering the change of momentum and velocity at the free inlet. The general equation of the dynamic motion of the OTEC CWP in the previous work was adapted[7]. Then the inlet boundary conditions were modified following the descriptions proposed by Païdoussis et al. [18]. The equation obtained was then solved using the Finite Element Method (FEM) by transferring it into its virtual energy form and solved in time domain analysis. The results have obtained and generally pointed out that the force balance at the inlet stabilized the pipe.

1.1 Material Selection for OTEC CWP

The main loads on the CWP and their trigger are listed in Table 2 [19]. In addition, the pipe is also subjected to the internal flow effect, which is separately discussed in the following subchapter. Table 2 shows that the characteristics of OTEC CWP must include high durability, toughness, lightness, chemical resistance, and high-pressure tolerance[20]. Resources from literature reviews[19,20] and based on experiences in other applications in which the typical loads of OTEC CWP apply, composite material is the most suitable candidate[21,22].

Table 2. Loading parameters for material selection.

Type of Loading	Cause
Fatigue strain	Plantship motion
Axial strain	Clump weight, wet weight
Bending strain	Current
Seawater corrosion	Lifespan
Pressure	1000m depth

The intended material properties can be obtained using composite material by optimizing the fiber volume fractions[23], layer components[24], reinforcement[25], and fabrication method[26].

Previous studies also examined the possibility of utilizing composites as the OTEC CWP material and found that the characteristics and material properties meet the OTEC requirement[19]. Thus, the composite material was used for the full-scale model analysis.

1.2 OTEC CWP as Pipe Conveying Fluid

Considering the characteristic of the CWP, it can be analyzed following the principle of top-tensioned pipe conveying fluid. Initially, Adiputra and Utsunomiya[10] included the internal flow effect in the design consideration. Nevertheless, the drag force was simplified to be linear and independent of the motion frequency. In the subsequent study, Adiputra and Utsunomiya[7] redefined the drag component by using an analytical analysis with two definitions of the drag force equation in the time and frequency domains. The definitions were considered to generate linear and non-linear dynamic equations of the pipe motion.

However, a contradiction occurs between analytical prediction and experiments regarding the dynamic stability of free-hanging pipe conveying fluid. The analytical theory predicts instability beyond a relatively small critical velocity value, while the experiment states otherwise[18,27,28].

To explain this contradiction, Kuiper and Metrikine[29] and Kuiper et al.[30] stated that the significant stabilizing factor on the pipe was the external hydrodynamic drag. Païdoussis et al.[18] and Giacobbi et al. [31] proposed several descriptions of the boundary condition for the transverse balance forces at the free end of the pipe by setting the pipe in a 'free-hanging' condition allowing the change of external and internal flow fields at the inlet. The difference between the velocity of external flow and internal flow may lead to a change of momentum and can further affect the stability of the riser.

In the most recent study by Adiputra and Utsunomiya[15], Finite Element Modeling was developed to investigate the dynamic behavior of riser conveying fluid in time-domain analysis. The result supported the theory that the riser should be unstable beyond its critical value.

However, based on experiment results reported by Hisamatasu et al. [32], the pipe was still stable at a velocity of two m/s. The fluid velocity of the experiment could not reach the critical value predicted by the theory due to the experiment facility limitation and high pressure lost along the pipe caused by friction between the internal flow and the riser. Thus, the critical velocity predicted by the analytical equation could not be explicitly proven. As a solution, the dynamic motions obtained from the experiment were compared analytically with the developed theory and numerically by utilizing the software Orcaflex. The result showed that the riser motion obtained from the experiment was far lower than the result obtained from Orcaflex, indicating that the critical velocity would be higher than the predicted one.

The results from Adiputra and Utsunomiya[15] and Hisamatasu et al.[32] showed more clearly that there was a gap between the theory and experiment regarding the dynamic motion of the riser conveying fluid.

In the previous research results[15], the full-scale model of OTEC CWP was predicted to lose stability in a `weak` state, so the critical value would be difficult to be observed in the time domain. Here, to better understand the influence of momentum change on the stability of the CWP and determine the critical velocity more accurately, the scaled model with the same OTEC CWP characteristic was employed as a small-scale model expected to result in `strong` instability. Then the full-scale model was investigated by repeating the procedures for the small-scale model.

2. Method

As mentioned, the Ocean Thermal Energy Conversion (OTEC) Cold Water Pipe (CWP) can be addressed as a free-hanging riser conveying fluid. The developed theories predict that such a riser should be unstable when the internal fluid velocity is above its critical value, either oscillatory or statically. Here, the stability of OTEC CWP was investigated analytically more accurately by considering the force balance at the inlet, as found in the numerical analysis using Finite Element Method (FEM).

In the first step, the general equation portraying the dynamic behavior of OTEC CWP was adapted from the previous studies and then transferred into virtual energy forms. The force balance descriptions were included by modifying the local stiffness and damping matrixes at the bottom-end node. After inducing boundary conditions in the global matrices, the system was solved using a Newmark time-scheme method.

Initially, the general equation was adapted as[7]

$$EI\frac{\partial^4 w}{\partial z^4} - 2u_f m_f \frac{\partial^2 w}{\partial t \partial z} + m_f {u_f}^2 \frac{\partial^2 w}{\partial z^2} + (m_f + m_r + m_a)\frac{\partial^2 w}{\partial t^2} - T_{BT}\frac{\partial^2 w}{\partial z^2} + T_{BT}\frac{Z}{L}\frac{\partial^2 w}{\partial z^2} + \frac{T_{BT}}{L}\frac{\partial w}{\partial z} + \frac{2\sqrt{2}}{\sqrt{\omega {r_o}^2/\upsilon}}\rho_f A_o \omega \frac{dw}{dt} = 0 \quad (1)$$

EI is the flexural rigidity of the pipe with length L, mass per unit m_r, and outer cross-sectional area A_o. The flow of the transported seawater is considered to move in a plug flow motion with constant velocity u_f and mass m_f causing the pipe to displace $w(z,t)$ at time t and distance z from the top-end of the pipe. Due to ambient fluid, the pipe is subjected to added mass m_a and motion frequency ω.

Accommodating the inflow direction effect and the flow field changes below the entrance, the shear force equilibrium at the inlet defined by Paidoussis et al. [29] was considered as Eqs. 2-4.

$$EI\frac{\partial^3 w}{\partial z^3} = 0 \quad (2)$$

$$EI\frac{\partial^3 w}{\partial z^3} - u_f m_f \frac{dw}{dt} = 0 \quad (3)$$

$$EI\frac{\partial^3 w}{\partial z^3} - u_f m_f\left(\frac{dw}{dt} - u_f\frac{\partial w}{\partial z}\right) = 0 \qquad (4)$$

For convenience, from here onward, the $u_f m_f \frac{dw}{dt}$ part will be mentioned as C_L and $m_f {u_f}^2 \frac{\partial w}{\partial z}$ as K_L. The next step is separating the t and z variables by assuming that $w(z,t)$ consists of two independent functions as

$$w(z,t) = \Delta^T(t)N(z) \qquad (5)$$

In the FEM, the $N(z)$ can be approached by a shape function. Here refers to the well-known Hermite shape function as[33,34)]

$$N(z) = \begin{bmatrix} (1-x/h)\text{^}2\,(1+2x/h) \\ -(1-x/h)\text{^}2\,x/h \\ (x/h)\text{^}2\,(3-2h/l) \\ (1-h/l)(h/l)\text{^}2 \end{bmatrix} \qquad (6)$$

h is the length of the element and x is the distance between the considered point on the pipe in local coordinate. Inserting Eq. 5 and Eq. 6 into Eq. 1 and converting it into its virtual energy form in the local coordinate system of riser element, Eq. 1 yields

$$\int_{t1}^{t2}\int_0^L (m_f + m_r + m_a)NN^T\ddot{\Delta}^T\partial\Delta^T dzdt + \int_{t1}^{t2}\int_0^L \left(2u_f m_f N`N^T + \frac{2\sqrt{2}}{\sqrt{\omega {r_o}^2/\upsilon}}\rho_f A_o \omega NN^T - u_f m_f [NN^T]_L\right)\dot{\Delta}^T\partial\Delta^T dzdt + \int_{t1}^{t2}\int_0^L \left(EIN````N^T + m_f {u_f}^2 N``N^T + \left[-T_{BT}\left(1-\frac{Z}{L}\right)\right]N``N^T + \frac{T_{BT}}{L}N`N^T + m_f {u_f}^2 [N`N^T]_L\right) dz\Delta^T\partial\Delta^T dt = 0 \qquad (7)$$

Then, the C_L and K_L terms are also transferred into its virtual energy form as $\overline{C_{e_L}} = -u_f m_f [NN^T]_L\dot{\Delta}^T$ and $\overline{K_{e_L}} = m_f {u_f}^2 [N`N^T]_L\Delta^T$ respectively. Finally, Eq. 7 is solved semi-analytically using MATLAB in the time domain analysis via Newmark Method Time Scheme[35)], where the acceleration is considered constant for a particular time step resulting in the motion velocity and displacement at a specific time step as

$$\dot{\Delta}_{i+1} = \dot{\Delta}_i + [(1-\gamma)(t_{i+1}-t_i)]\ddot{\Delta}_i + \gamma(t_{i+1}-t_i)\ddot{\Delta}_{i+1} \qquad (8)$$

$$\Delta_{i+1} = \Delta_i + (t_{i+1}-t_i)\dot{\Delta}_i + \left[(0.5-\beta)(t_{i+1}-t_i)^2\right]\ddot{\Delta}_i + \beta(t_{i+1}-t_i)^2\ddot{\Delta}_{i+1} \qquad (9)$$

The value of parameter γ is set as 0.25, and the value of parameter β is set as 0.5 following constant acceleration. Initially, a nodal force is imposed at all nodes of the elements along the pipe then the force is released. If the system is stable, the pipe will displace and gradually return to the static condition. However, if the system is unstable, the motion amplitude will increase either oscillatory or statically.

3. Small Scale Model

The numerical setup for the simulation is listed in table 3. The parameters for the small-scale model were adopted from the previous study[15)], as listed in Table 4 for the pipe scantling and Table 5 for the material properties. The stability was analyzed using a small-scale pipe model fixed at the top and free at the bottom end of the pipe. The internal fluid velocities were increased incrementally, and the last node displacement graph was obtained for each velocity value. Case one refers to the condition where C_L and K_L are neglected as Eq. 2, case two indicates that only C_L is considered as Eq. 3, and case three means both are considered as Eq. 4.

Table 3. Numerical simulation setup

Parameter	**Small-scale**
Number of elements	50
Initial force	1.0 E-3 N
Total time 1 m/s velocity 2 m/s velocity ≥ 3 m/s Velocity	 50 s 100 s 500 s
Timestep	1.0E-3

Table 4. Small pipe scantlings.

Parameter	**Scantling**
Length of the pipe	4 m
Inner diameter of the pipe	20 mm
Outer diameter of the pipe	22 mm

Table 5. Properties of the small pipe simulation.

Parameter	**Properties**
Density of the pipe	1238 kg/m^3
Modulus elasticity of the pipe	2.8E9 Pa
Outer diameter of the pipe	1000 kg/m^3

The responses of pipe motion for all cases were observed at velocities of 1 m/s and 2 m/s, as shown in Fig. 2 and Fig. 3. The Y- axis is the response of the displacement at the bottom end of the pipe in meter and X- axis is the timestep. The green line shows the bottom end displacement of case one, the blue line for case two, and the red line for case three.

From Fig. 2, it can be seen that the displacement amplitude spiked up and decreased significantly in a short time from the release of the initial force. A slight flutter in the first 10 seconds of the time step was also observable,

particularly in case one. Then, the system went back to the static, stable condition immediately.

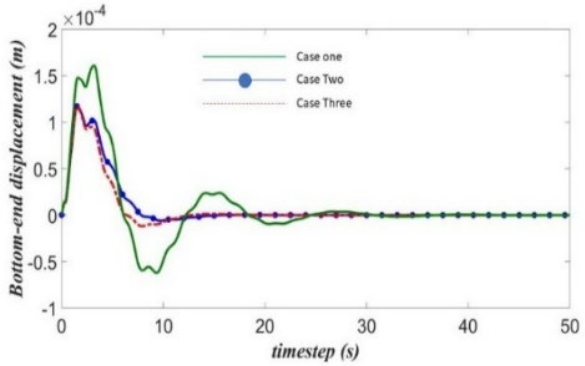

Fig. 2: Small pipe response at u_f of 1.0 m/s.

Fig. 3 shows that system was stable despite the high amplitude in the early step. After the initial force was released, all lines showed an increase in amplitude, whereas case 1 was observed to have the highest one. The vibration amplitude then decayed and the pipe returned to a stable condition. With the increase of fluid velocity reaching relatively higher values, the response for each case was unique. Thus, for clarity, the critical velocity analysis will be done for each particular case separately.

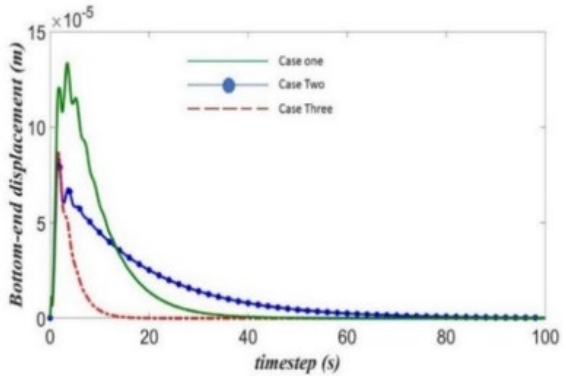

Fig. 3: Small pipe response at u_f of 2.0 m/s.

3.1 Critical Velocity Estimation for Case One

Figs. 4-6 plot the pipe response at around its critical values covering velocities of 2.3 m/s, 2.4 m/s, and 2.32 m/s, respectively. As shown in Fig. 4, at a velocity of 2.3 m/s, the system was still in stable condition, where a small amount of flutter took place before returning to the stable state. Compared to Fig. 2 and Fig. 3, where internal flow velocities were 1 m/s and 2 m/s, the system had higher motion amplitude and a longer time required to return to its stable condition.

The instability was observed at a velocity of 2.4 m/s, as shown in Fig. 5, pointed out by the increase in pipe response. The system was in static instability condition with no flutter, yet the displacement significantly increased. Up to this step, critical velocity can be predicted between 2.3-2.4 m/s.

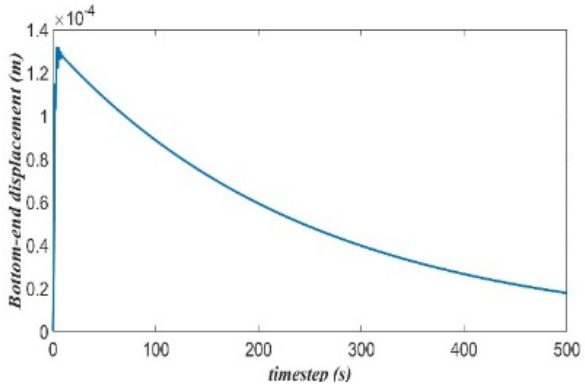

Fig. 4: Small pipe response for case 1 at u_f of 2.3 m/s.

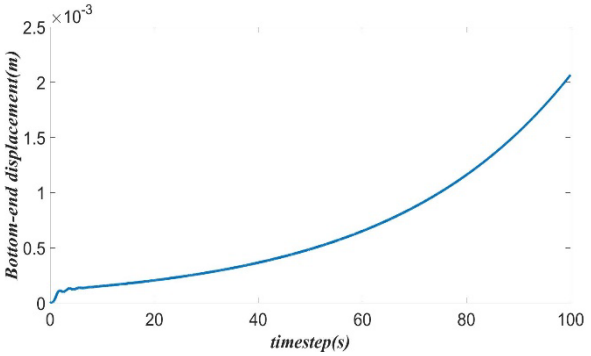

Fig. 5: Small pipe response for case 1 at u_f of 2.4 m/s.

For cautious investigation, the next analysis used a flow rate increment of 0.2 m/s starting from 2.3 m/s. The instability occurred at the velocity of 2.32 m/s, as shown in Fig. 6. After the initial force was released, the flutter took place with a slight amplitude increase. At the time that the system converges, the rise in amplitude was clearly visible.

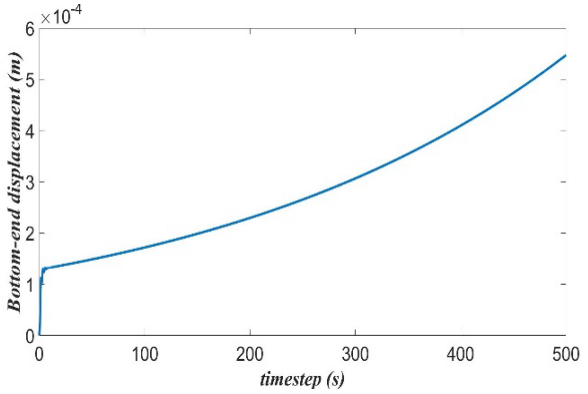

Fig. 6: Small pipe response for case 1 at u_f of 2.32 m/s.

3.2 Critical Velocity Estimation for Case Two

The analysis procedure used in case one was duplicated to analyze case two. In general, the results of case two also showed the same tendency as case one. Figs. 7-9 plots the pipe response for case two at around its critical values covering velocities of 2.3 m/s, 2.4 m/s, and 2.32 m/s.

Fig. 7 shows that the system at a fluid velocity of 2.3 m/s first reaches high amplitude and then decayed flutter

in a concise amount of time while Fig. 8 indicates that fully static instability occurred at a velocity of 2.4 m/s.

A denser fluid velocity increment was carried out, resulting in the critical velocity being 2.32 m/s as shown in Fig. 9. The system first flutters and then got unstable with a relatively linear increment of bottom-end node displacement.

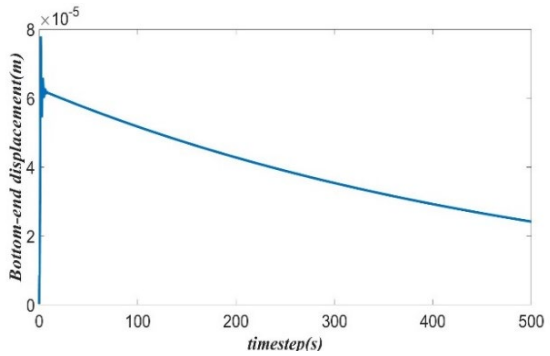

Fig. 7: Small pipe response for case 2 at u_f of 2.3 m/s.

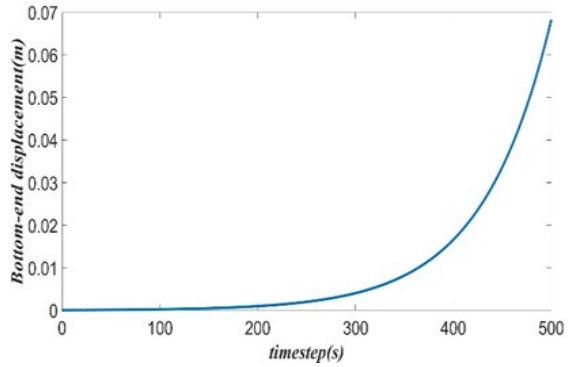

Fig. 8: Small pipe response for case 2 at u_f of 2.4 m/s.

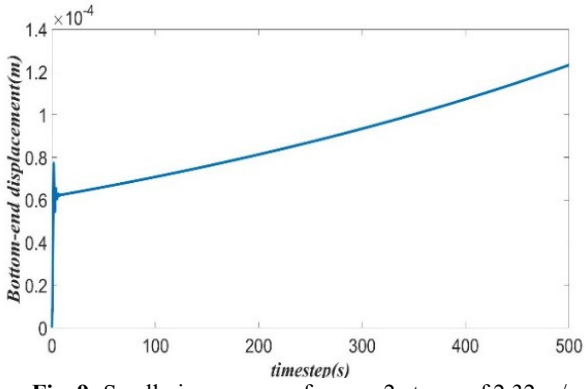

Fig. 9: Small pipe response for case 2 at u_f of 2.32 m/s.

3.3 Critical Velocity Estimation for Case Three

In case three, even the system vibrates with a slighter decrease of motion amplitude and a more extended period to return to its initial state, it was still stable up to 5 m/s, as shown in Fig. 9. The pipe fluttered with decaying amplitude.

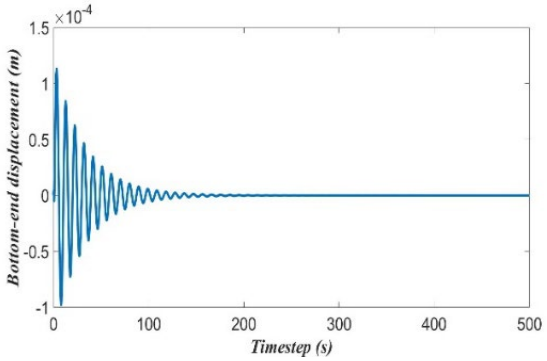

Fig. 10: Small pipe response for case 3 at u_f of 5 m/s.

However, by increasing the fluid velocity to 5.1 m/s, only 0.1 m/s increased from the previous analysis, the response of the pipe already shows instability, as shown in Fig 11. The vibration amplitude increased along with the timestep increment by means that negative damping occurs. Therefore, the critical velocity can be obtained from the 5-5.1 m/s range.

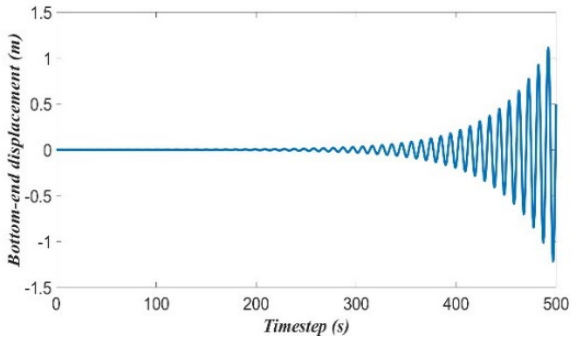

Fig. 11: Small pipe response for case 3 at u_f of 5.1 m/s.

A more refined analysis using a flow rate of 5.05 m/s was calculated, resulting in Fig. 12. the system was still stable at this condition.

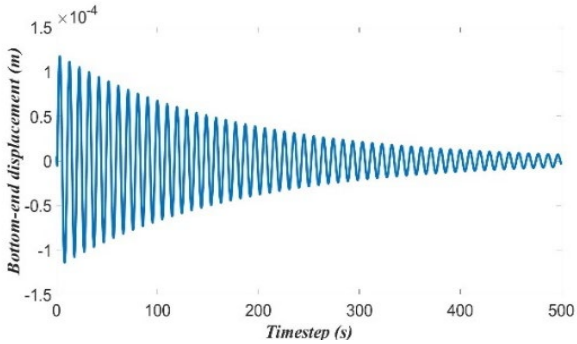

Fig. 12: Small pipe response for case 3 at u_f of 5.05 m/s.

For further analysis, another increment of 0.01 m/s fluid velocity was added to the analysis resulting in Fig. 13. At a velocity of 5.06 m/s, the system was stable but very close to onset instability; the system kept vibrating with a slight decrease of the vibration amplitude by timestep. The critical value is obtained here.

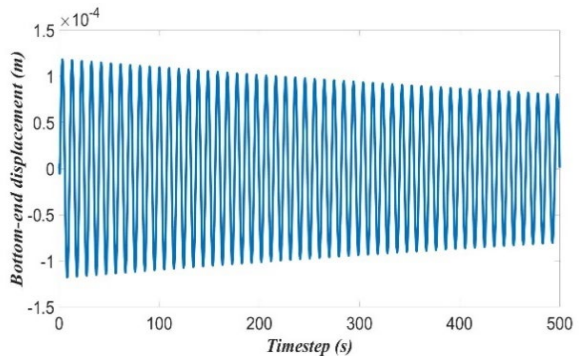

Fig. 13: Small pipe response for case 3 at u_f of 5.06 m/s.

3.4 Discussion on the small-scale results

The critical velocity had been obtained as listed in Table 6, and the tendency of the pipe response due to the increase of the internal fluid velocity had also been observed for all cases.

Table 6. Critical velocity

Case	Critical velocity
1	2.32 m/s
2	2.32 m/s
3	5.06 m/s

From Table 6, it is concluded that for case one and case two, the tendency of the pipe response was similar, resulting in the same critical velocity of around 2.32 m/s. It can be pointed out that C_L term did not significantly influence the pipe response as its inclusion and the negligence of this term did not change the pipe response. However, comparing cases one and two with case three, the critical velocity became 5.06 m/s, twice higher than cases 1 and 2. It showed that the K_L term significantly increased damping force of the system so that the pipe can be stable at higher fluid velocity.

4. Full Scale Model

The material for the full-scale model was FRP with properties listed in Table. 7.

Table 7. FRP Properties

Parameters	Scantling
Inner diameter	3 m
Thickness	6 cm
Length	1000 m
Young`s modulus	9000 MPa
Density	1238 Kg/m^3

The method and the analysis procedures for the small-scale model will be carried out for the full-scale model. For each case, the seawater transport velocity was increased with an increment of 1 m/s and decreased gradually near the critical velocity. In the analysis, the pipe was divided into 100 elements with a total time of 1000 and a time increment of 1.

To investigate how the boundary condition at the top joint influenced the critical velocities, in the full-scale analysis, the connection between the CWP and the platform varies to be in the pinned joint and fixed joints. The obtained critical velocities are shown in Table 8.

Table 8. Critical velocity in m/s for Full-scale model

	Fixed joint	Pinned joint
Case 1	3.66	3.58
Case 2	3.68	3.62
Case 3	5	4.75

Table 8 shows that the critical velocity of the full-scale OTEC CWP also increased with the inclusion of the K_L term. The effect of the top joint connection on the critical velocity was also significant when the K_L term was included.

Considering all the results together, it can be seen that the force balance at the inlet of the pipe plays a significant role in the pipe stability as mentioned in the precious works stated in the introductions.

5. Conclusions

This paper has investigated the effect of variations in the shear force balance at the inlet, as in cases one, two, and three. The analysis was conducted using Finite Element Modelling (FEM), and the time-dependent function of the displacement equation was discretized using the Newmark time scheme. The critical velocity had been obtained. The tendency of pipe response due to internal fluid velocity increase had also been observed for all cases in the small-scale model analysis. The CWP actual size was first scaled down to simplify the investigation, and then the procedures were adopted for the full-scale model.

In general, it can be pointed out that C_L term did not significantly influence the pipe response but the K_L term significantly stabilized the pipe response. This analysis successfully proved that the critical velocity increased with the introduction of shear force balance at the inlet.

The stability analysis in the frequency domain which is preferable to portray the negative damping of the system will also be conducted in the future. A more accurate description of the general equation, the shear force balance, and the depressurization condition at the inlet is required to more precisely determine the Internal Flow Effects (IEF) on the pipe stability. Experiment capability on this typical configuration to conduct higher and more stable internal flow velocity is also demanded.

Acknowledgements

This work is part of the OTEC research activity

"Preliminary Design of a 5 MW OTEC plant: Study case in the North Bali" research grand DIPA-124.01.1.690505/2023 conducted by the Marine Renewable Energy Conversion Technology research group, Research Center for Hydrodynamics Technology, National Research and Innovation Agency (BRIN). Collaboration with the Laboratory of Design and Computational Mechanics, Universitas Sebelas Maret (UNS) is highly acknowledged.

Nomenclature

A_o	outer cross-sectional area
EI	flexural rigidity of the pipe
L	length of the pipe
m_a	added mass due to ambient fluid
m_f	mass of the transported fluid per unit length
m_r	mass of the pipe per unit length
r_o	outer radius of the pipe
T_{BT}	wet weight of the pipe
t	time
u_f	velocity of the transported fluid
$w(z,t)$	tranverese displacement
z	distance between the considered point with the top-end of the pipe

Greek symbols

υ	kinematic viscosity of the transported fluid
ω	motion frequency

References

1) W.H. Avery, "Ocean thermal energy conversion (OTEC)," Encycl. Phys. Sci. Technol., 123–160 (2003). doi:10.1016/B0-12-227410-5/00511-1.
2) G.C. Nihous, "A preliminary assessment of ocean thermal energy conversion resources," J. Energy Resour. Technol. Trans. ASME, 129 (1) 10–17 (2007). doi:10.1115/1.2424965.
3) M.L. Syamsuddin, A. Attamimi, A.P. Nugraha, S. Gibran, A.Q. Afifah, and N. Oriana, "OTEC potential in the indonesian seas," Energy Procedia, 65 215–222 (2015). doi:10.1016/J.EGYPRO.2015.01.028.
4) R. Adiputra, and T. Utsunomiya, "Design optimization of floating structure for a 100 MW-net ocean thermal energy conversion (OTEC) power plant," in: Proc. Int. Conf. Offshore Mech. Arct. Eng. - OMAE, 2018. doi:10.1115/OMAE2018-77539.
5) C. Bernardoni, M. Binotti, and A. Giostri, "Techno-economic analysis of closed otec cycles for power generation," Renew. Energy, 132 1018–1033 (2019). doi:10.1016/J.RENENE.2018.08.007.
6) R. Adiputra, T. Utsunomiya, J. Koto, T. Yasunaga, and Y. Ikegami, "Preliminary design of a 100 mw-net ocean thermal energy conversion (otec) power plant study case: mentawai island, indonesia," J. Mar. Sci. Technol., 25 (1) (2020). doi:10.1007/s00773-019-00630-7.
7) R. Adiputra, and T. Utsunomiya, "Linear vs non-linear analysis on self-induced vibration of otec cold water pipe due to internal flow," Appl. Ocean Res., 110 (2021). doi:10.1016/j.apor.2021.102610.
8) R. Adiputra, and T. Utsunomiya, "Stability based approach to design cold-water pipe (cwp) for ocean thermal energy conversion (otec)," Appl. Ocean Res., 92 (2019). doi:10.1016/j.apor.2019.101921.
9) O.M. Griffin, "Otec cold water pipe design for problems caused by vortex-excited oscillations," Ocean Eng., 8 (2) 129–209 (1981). doi:10.1016/0029-8018(81)90023-8. 1)
10) R. Adiputra, and T. Utsunomiya, "Stability analysis of free hanging riser conveying fluid for ocean thermal energy conversion (OTEC) utilization," in: Proc. Int. Conf. Offshore Mech. Arct. Eng. - OMAE, 2019. doi:10.1115/OMAE2019-96749.
11) R. Hisamatsu, and T. Utsunomiya, "Coupled response characteristics of cold water pipe and moored ship for floating otec plant," Appl. Ocean Res., 123 103151 (2022). doi:10.1016/J.APOR.2022.103151.
12) W. S. Edelstein, S. S.Chen, & J. A. Jendrzejczyk, "A finite element computation of the flow-induced oscillations in a cantilevered tube, " Journal of Sound and Vibration, 107 (1), 121-129 (1986). doi: 10.1016/0022-460X(86)90287-7
13) M. Langthjem, "Finite element analysis and optimization of a fluid-conveying pipe. Mechanics of Structures and Machines," 23(3), 343-376 (1995). doi: 10.1080/08905459508905242.
14) J. Leklong, S. Chucheepsakul, & S. Kaewunruen,. "Dynamic responses of marine risers/pipes transporting fluid subject to top end excitations," In The Eighth ISOPE Pacific/Asia Offshore Mechanics Symposium. 2008. OnePetro.
15) R. Adiputra, and T. Utsunomiya, "Finite element modelling of ocean thermal energy conversion (otec) cold water pipe (cwp)," in: Proc. Int. Conf. Offshore Mech. Arct. Eng. - OMAE, 2022. doi:10.1115/OMAE2022-78135.
16) R. Hisamatsu, & T. Utsunomiya, "Free Vibration and Stability of a Fully Submerged Pipe Aspirating Fluid: An Experiment and New Physical Insights, " Journal of Fluids and Structures, 116, 103789 2022. doi: 10.2139/ssrn.4174747
17) J. Langer, C. Infante Ferreira, and J. Quist, "Is bigger always better? designing economically feasible ocean thermal energy conversion systems using spatiotemporal resource data," Appl. Energy, 309 118414 (2022). doi:10.1016/J.APENERGY.2021.118414.
18) M.P. Païdoussis, C. Semler, and M. Wadham-Gagnon, "A reappraisal of why aspirating pipes do not flutter

at infinitesimal flow," J. Fluids Struct., 20 (1) 147–156 (2005). doi:10.1016/J.JFLUIDSTRUCTS.2004.09.004.
19) A. Miller, and M. Ascari, "OTEC Advanced Composite Cold Water Pipe: Final Technical Report," United States, 2011. doi:10.2172/1024183.
20) M. Dalil, B. Wirjosentono, J. Koto, and A. Ginting, "Load characteristics of cold water pipe based on fibreglass-filled hdpe composites," AIP Conf. Proc., 2342 (1) 60005 (2021). doi:10.1063/5.0046393.
21) A.M.M. Ismaiel, S.M. Metwalli, B.M.N. Elhadidi, and S. Yoshida, "Fatigue analysis of an optimized hawt composite blade," Evergreen, 4 (2–3) 1–6 (2017). doi:10.5109/1929656.
22) R. Scotti, and T. McGuinness, "Design and analysis of OTEC's cold water pipe," United States, 1980. https://www.osti.gov/biblio/6726919.
23) M.R. Zakaria, M.F. Omar, H.M. Akil, and M.M.A.B. Abdullah, "Study of carbon nanotubes stability in different types of solvents for electrospray deposition method," Evergreen, 7 (4) 538–543 (2020). doi:10.5109/4150473.
24) A. Kumar, A.K. Chanda, and S. Angra, "Numerical modelling of a composite sandwich structure having non metallic honeycomb core," Evergreen, 8 (4) 759–767 (2021). doi:10.5109/4742119.
25) D. Choudhari, and V. Kakhandki, "Characterization and analysis of mechanical properties of short carbon fiber reinforced polyamide66 composites," Evergreen, 8 (4) 768–776 (2021). doi:10.5109/4742120.
26) A. Gupta, H. Kumar, L. Nagdeve, and P.K. Arora, "EDM parametric study of composite materials: a review," Evergreen, 7 (4) 519–529 (2020). doi:10.5109/4150471.
27) G.L. Kuiper, and A. V. Metrikine, "Experimental investigation of dynamic stability of a cantilever pipe aspirating fluid," J. Fluids Struct., 24 (4) 541–558 (2008). doi:10.1016/J.JFLUIDSTRUCTS.2007.10.011.
28) M.P. Païdoussis, and N.T. Issid, "Dynamic stability of pipes conveying fluid," J. Sound Vib., 33 (3) 267–294 (1974). doi:10.1016/S0022-460X(74)80002-7.
29) G.L. Kuiper, and A. V. Metrikine, "Dynamic stability of a submerged, free-hanging riser conveying fluid," J. Sound Vib., 280 (3–5) 1051–1065 (2005). doi:10.1016/J.JSV.2004.09.024.
32) R. Hisamatsu, R. Adiputra, and T. Utsunomiya, "Experimental study on dynamic characteristics of fluid-conveying pipe for otec," in: Proc. Int. Conf. Offshore Mech. Arct. Eng. - OMAE, 2022. doi:10.1115/OMAE2022-78136.
30) G.L. Kuiper, A. V. Metrikine, and J.A. Battjes, "A new time-domain drag description and its influence on the dynamic behaviour of a cantilever pipe conveying fluid," J. Fluids Struct., 23 (3) 429–445 (2007). doi:10.1016/J.JFLUIDSTRUCTS.2006.09.007.
31) D.B. Giacobbi, S. Rinaldi, C. Semler, and M.P. Païdoussis, "The dynamics of a cantilevered pipe aspirating fluid studied by experimental, numerical and analytical methods," J. Fluids Struct., 30 73–96 (2012). doi:10.1016/J.JFLUIDSTRUCTS.2011.11.011.
32) R. Hisamatsu, R. Adiputra, and T. Utsunomiya, "Experimental study on dynamic characteristics of fluid-conveying pipe for otec," in: Proc. Int. Conf. Offshore Mech. Arct. Eng. - OMAE, 2022. doi:10.1115/OMAE2022-78136.
33) C.E. Augarde, "Generation of shape functions for straight beam elements," Comput. Struct., 68 (6) 555–560 (1998). doi:10.1016/S0045-7949(98)00071-6.
34) J. Yarasca, J.L. Mantari, and R.A. Arciniega, "Hermite–lagrangian finite element formulation to study functionally graded sandwich beams," Compos. Struct., 140 567–581 (2016). doi:10.1016/J.COMPSTRUCT.2016.01.015.
35) S. Krenk, "Energy conservation in newmark based time integration algorithms," Comput. Methods Appl. Mech. Eng., 195 (44–47) 6110–6124 (2006). doi:10.1016/J.CMA.2005.12.001.